

Sparse time-varying parameter VECMs with an application to modeling electricity prices

NIKO HAUZENBERGER¹, MICHAEL PFARRHOFER¹ and LUCA ROSSINI^{2*}

¹*University of Salzburg*

²*Queen Mary University of London*

In this paper we propose a time-varying parameter (TVP) vector error correction model (VECM) with heteroscedastic disturbances. We combine a set of econometric techniques for dynamic model specification in an automatic fashion. We employ continuous global-local shrinkage priors for pushing the parameter space towards sparsity. In a second step, we post-process the cointegration relationships, the autoregressive coefficients and the covariance matrix via minimizing Lasso-type loss functions to obtain truly sparse estimates. This two-step approach alleviates overfitting concerns and reduces parameter estimation uncertainty, while providing estimates for the number of cointegrating relationships that varies over time. Our proposed econometric framework is applied to modeling European electricity prices and shows gains in forecast performance against a set of established benchmark models.

JEL: C11, C32, C53, Q40

KEYWORDS: Cointegration, reduced rank regression, sparsification, hierarchical shrinkage priors, error correction models

**Corresponding author:* Luca Rossini. *Email:* l.rossini@qmul.ac.uk. We thank Florian Huber for valuable comments and suggestions. Hauzenberger and Pfarrhofer gratefully acknowledge financial support from the Austrian Science Fund (FWF, grant no. ZK 35) and the Oesterreichische Nationalbank (OeNB, Anniversary Fund, project no. 18127).

1. INTRODUCTION

In this paper we propose a time-varying parameter (TVP) vector error correction model (VECM) with heteroscedastic disturbances. We introduce a set of econometric novelties for dynamic and automatic model specification, and apply these methods to modeling European electricity prices.

The estimation of VECMs, particularly with TVPs, poses several challenges (see also Koop *et al.*, 2011). First, there is often no compelling a priori argument how a set of variables are cointegrated, especially in high-dimensions. And this complicates introducing reasonable restrictions to identify the long-run behavior of observed series. Second, and relatedly, the cointegration rank is unknown and subject to change depending on the specific application.¹ Third, large TVP models are prone to overfitting. A large number of papers propose to restrict the parameter space relying on hierarchical prior distributions or approximations.²

Our approach combines several recent econometric advances for large-scale TVP models and reduced-rank regressions. This allows us to circumvent many of the above mentioned issues for estimating TVP-VECMs in an automatic fashion. First, we employ continuous global-local shrinkage priors for pushing the parameter space towards sparsity. However, as noted by Chakraborty *et al.* (2020), such priors solely achieve approximate zeroes, and the probability of observing exact zeroes is zero. As a remedy, we post-process our posterior draws via minimizing Lasso-type loss functions to obtain sparse estimates for the cointegration matrix, the autoregressive parameters and the covariance matrix (see also Hahn and Carvalho, 2015; Ray and Bhattacharya, 2018). A key novelty of our framework is that it selects the number of cointegration relationships for each period. Additionally, sparsifying the draws ex post alleviates overfitting concerns and reduces parameter estimation uncertainty (see Huber *et al.*, 2020a).

To assess the merits of the proposed framework we apply our methods to modeling electricity prices in several European countries. Deregulation and increasingly competitive markets in the power sector have led to a surge of interest in statistical methods for modeling and forecasting electricity demand and price dynamics. Competing approaches include both univariate and multivariate time-series models in linear and nonlinear settings. For an overview of the related literature, see Weron (2014). Most directly related to our approach, De Vany and Walls (1999) show that electricity prices in US states are strongly cointegrated, with long-run relationships driven by no-arbitrage conditions. The more recent literature typically also finds strong evidence of common dynamics and cointegration relationships between electricity and gas prices for major power exchanges in the European Union (see Bosco *et al.*, 2010; Houllier and De Menezes, 2012; Bello and Reneses, 2013; De Marcos *et al.*, 2016; Gianfreda *et al.*, 2019).

In light of this empirical evidence, our econometric approach thus features several attractive properties that are required to successfully trace the evolution of energy prices. First,

¹ The previous literature often conditions on the rank and compares marginal likelihoods or predictive performance ex post. Notable exceptions are Jochmann and Koop (2015) and Chua and Tsiaplias (2018), who use regime-switching models to estimate time-varying cointegration ranks. These papers either use rather small information sets, or introduce strong prior information on the cointegration rank. Both limitations are often impractical and identifying restrictions on the cointegration relationships can be tedious in large-scale models from an applied perspective.

² Relevant contributions in this context are Bunea *et al.* (2012), Jochmann *et al.* (2013), Eisenstat *et al.* (2016), Huber and Zörner (2019), Chakraborty *et al.* (2020), Hauzenberger *et al.* (2020a,c), Huber *et al.* (2020b).

VECMs allow for discriminating between long-run equilibria and short-run adjustment dynamics. This feature might be useful to uncover cointegrating relationships between countries, or complex equilibrium dynamics among intra-day prices. Second, TVPs capture structural breaks in the dynamic relationships of the underlying data. This may be particularly useful for addressing complex latent pricing mechanisms and varying importance of variables such as fuel prices that may be subject to change over time. Third, using our shrink-then-sparsify approach allows for variable selection in high-dimensional datasets. Finally, heteroscedastic errors capture large unanticipated shocks in prices, a crucial feature when interest centers on producing accurate density forecasts (see, for instance, [Gianfreda *et al.*, 2020](#)).

We provide two empirical applications. First, we illustrate our approach using daily data across several European economies. Our proposed procedure yields estimates for the cointegration rank that vary over time. Moreover, we detect several interesting patterns of sparsity in both dynamic and static interdependencies in energy markets. And we find that while heavy tailed errors are required for modeling electricity prices in some European countries, this feature is less important in others. Second, we conduct an extensive out-of-sample forecast exercise for hourly electricity prices for Germany. We consider forecasts for each hour of the following day. We find that multivariate models with TVPs and heteroscedastic errors provide improvements relative to simpler univariate benchmarks. In particular, the forecast exercise indicates that our proposed sparsified TVP-VECM performs well for predictive inference on German electricity prices.

The rest of the paper is organized as follows. Section 2 introduces the TVP-VECM. We discuss related identification issues, and propose a parsimonious framework for dynamically selecting time-varying cointegration ranks. Section 3 applies the TVP-VECM to modeling European electricity prices. Section 4 summarizes and concludes the paper.

2. ECONOMETRIC FRAMEWORK

2.1. The TVP-VECM

Let \mathbf{y}_t be an $M \times 1$ -dimensional vector of endogenous variables for $t = 1, \dots, T$, and denote the first difference operator by Δ . A general specification of the TVP-VECM of order P is

$$\Delta \mathbf{y}_t = \mathbf{\Pi}_t \mathbf{w}_t + \sum_{p=1}^P \mathbf{A}_{pt} \Delta \mathbf{y}_{t-p} + \gamma_t \mathbf{c}_t + \boldsymbol{\epsilon}_t, \quad \boldsymbol{\epsilon}_t \sim \mathcal{N}(\mathbf{0}, \boldsymbol{\Sigma}_t). \quad (1)$$

Here, $\mathbf{w}_t = (\mathbf{y}'_{t-1}, \mathbf{f}'_{t-1})'$, where \mathbf{y}_{t-1} is the first lag of the endogenous vector and \mathbf{f}_{t-1} is a set of q_f exogenous factors such that \mathbf{w}_t is of size $q \times 1$ with $q = M + q_f$. $\mathbf{\Pi}_t$ is an $M \times q$ -dimensional matrix of reduced rank $r_t < M$. \mathbf{A}_{pt} refers to an $M \times M$ time-varying coefficient matrix for the p th lag $\Delta \mathbf{y}_{t-p}$, and γ_t of size $M \times N$ relates an $N \times 1$ -vector \mathbf{c}_t of deterministic terms (such as seasonal dummies, trends or intercepts) to $\Delta \mathbf{y}_t$. We assume a zero mean Gaussian error term $\boldsymbol{\epsilon}_t$ with time-varying $M \times M$ -covariance matrix $\boldsymbol{\Sigma}_t$.

The cointegration matrix

A more thorough discussion of the matrix $\mathbf{\Pi}_t$ of reduced rank r_t , governing the cointegration relationships, is in order. In most applications using VECMs, $r_t = \bar{r}$ is some time-invariant fixed integer with $1 \leq \bar{r} \leq (M - 1)$. The rank order is commonly motivated either based on economic theory (see, for instance, [Giannone et al., 2019](#)), or “estimated” by calculating marginal likelihoods for a set of possible ranks (see [Geweke, 1996](#)). For large-scale models, such approaches are often computationally prohibitive. As a solution, we adapt the approach of [Chakraborty et al. \(2020\)](#) for the TVP-VECM and estimate r_t for each period.

It is convenient to consider a parameter expanded framework ([Liu and Wu, 1999](#); [Chakraborty et al., 2020](#)), $\mathbf{\Pi}_t = \boldsymbol{\alpha}_t \boldsymbol{\beta}'$. Here, the short-run adjustment coefficients are collected in $\boldsymbol{\alpha}_t$ of dimension $M \times q$ and the long-run relationships are captured by $\boldsymbol{\beta}$ which is $q \times q$. Note that we follow [Yang and Bauwens \(2018\)](#) and assume the long-run relations to be constant over time.³ This amounts to the comparatively uncontroversial assumption that long-run fundamental relations do not change over time and our interest centers on the combined matrix $\mathbf{\Pi}_t$, where nonlinearities appear through $\boldsymbol{\alpha}_t$.

However, we refrain from restricting the cointegration space by imposing a deterministic structure on $\boldsymbol{\beta}$ (see also [Strachan, 2003](#); [Strachan and Inder, 2004](#); [Villani, 2006](#)). In particular, we follow [Koop et al. \(2009\)](#) and [Koop et al. \(2011\)](#) and use the transformations

$$\tilde{\boldsymbol{\alpha}}_t = \boldsymbol{\alpha}_t \boldsymbol{\zeta}^{-1}, \quad \tilde{\boldsymbol{\beta}} = \boldsymbol{\beta} \boldsymbol{\zeta}, \quad \text{with } \boldsymbol{\zeta} = (\tilde{\boldsymbol{\beta}}' \tilde{\boldsymbol{\beta}})^{-0.5}.$$

This allows for employing a linear state-space modeling approach assuming conditional Gaussianity with a cointegration space prior. Note that [Chakraborty et al. \(2020\)](#) do not specify a prior on the cointegration space, but rather specify independent standard normally distributed priors directly on the elements in $\boldsymbol{\beta}$.

Rewriting the state-space model for efficient estimation

We proceed by constructing the following vectors and matrices for notation simplicity:

$$\begin{aligned} \mathbf{A}_t &= (\mathbf{A}_{1t}, \dots, \mathbf{A}_{Pt}, \boldsymbol{\gamma}_t) \text{ of size } M \times J, \\ \mathbf{x}_t &= (\Delta \mathbf{y}'_{t-1}, \dots, \Delta \mathbf{y}'_{t-P}, \mathbf{c}'_t)' \text{ of size } J \times 1, \end{aligned}$$

where we define $J = (MP + N)$, $\mathbf{B}_t = (\tilde{\boldsymbol{\alpha}}_t, \mathbf{A}_t)$. Moreover, it is convenient to factorize $\boldsymbol{\Sigma}_t = \mathbf{L}_t \mathbf{H}_t \mathbf{L}_t'$, with $\mathbf{H}_t = \text{diag}(h_{1t}, \dots, h_{Mt})$ and \mathbf{L}_t denoting the normalized lower Cholesky factor. We rewrite the model to allow for equation-by-equation estimation (see, for instance, [Carriero et al., 2019](#)):

$$\Delta \mathbf{y}_t = \mathbf{B}_t \mathbf{z}_t + \mathbf{L}_t \boldsymbol{\eta}_t, \quad \boldsymbol{\eta}_t \sim \mathcal{N}(\mathbf{0}, \mathbf{H}_t),$$

³ Assuming both $\boldsymbol{\alpha}_t$ and $\boldsymbol{\beta}_t$ to vary over time further complicates achieving identification. First, note that $\mathbf{\Pi}_t = \boldsymbol{\alpha}_t \boldsymbol{\beta}_t' = \boldsymbol{\alpha}_t \mathbf{Q} \mathbf{Q}^{-1} \boldsymbol{\beta}_t'$ for any non-singular matrix \mathbf{Q} which results in the so-called global identification problem. It is common in the literature to use linear normalization schemes such as $\boldsymbol{\beta}_t = (\mathbf{I}_{r_t}, \boldsymbol{\beta}_t')'$, see also [Villani \(2001\)](#) or [Strachan \(2003\)](#). Second, the local identification problem appears for $\boldsymbol{\alpha}_t = \mathbf{0}$ which implies that $\text{rank}(\mathbf{\Pi}_t) = 0$ (see [Kleibergen and Van Dijk, 1994; 1998; Paap and Van Dijk, 2003](#)).

where $\tilde{\mathbf{w}}_t = \tilde{\beta}' \mathbf{w}_t$ and $\mathbf{z}_t = (\tilde{\mathbf{w}}_t', \mathbf{x}_t')'$. The i th equation of the system is given by

$$\Delta y_{it} = \mathbf{B}_{i\bullet,t} \mathbf{z}_t - \sum_{j=1}^{i-1} l_{ij,t}^{-1} \epsilon_{jt} + \eta_{it}, \quad \eta_{it} \sim \mathcal{N}(0, h_{it}).$$

Here, $\mathbf{B}_{i\bullet,t}$ denotes the i th row of \mathbf{B}_{it} , $l_{ij,t}$ refers to the j th element in the i th row of \mathbf{L}_t^{-1} . Collecting the terms, we may further simplify:

$$\Delta y_{it} = \mathbf{b}_{it}' \mathbf{Z}_{it} + \eta_{it} \quad (2)$$

by defining the $K_i \times 1$ -vectors $\mathbf{Z}_{it} = (\mathbf{z}_t', \{-\epsilon_{jt}\}_{j=1}^{i-1})'$ and $\mathbf{b}_{it} = (\mathbf{B}_{i\bullet,t}, \{l_{jt}^{-1}\}_{j=1}^{i-1})'$. For the TVPs, we assume a random walk law of motion:

$$\mathbf{b}_{it} = \mathbf{b}_{it-1} + \boldsymbol{\vartheta}_{it}, \quad \boldsymbol{\vartheta}_{it} \sim \mathcal{N}(\mathbf{0}, \boldsymbol{\Theta}_i), \quad (3)$$

with diagonal covariance matrix $\boldsymbol{\Theta}_i = \text{diag}(\theta_{i1}, \dots, \theta_{iK_i})$. To implement a stochastic volatility specification, the logarithm of the time-varying variances follow independent AR(1) processes,

$$\log h_{it} = \mu_i + \phi_i(\log h_{it-1} - \mu_i) + \varsigma_i \xi_{it}, \quad \xi_{it} \sim \mathcal{N}(0, 1), \quad (4)$$

where μ_i is the unconditional mean, ϕ_i , is the persistence parameter and ς_i is the error variance of the log-volatility process.

For our prior setup, we use the non-centered parameterization of the regression model (Frühwirth-Schnatter and Wagner, 2010). The methods proposed in this paper may be combined with any desired setup from the class of global-local shrinkage priors. From this class of priors, we choose the horseshoe prior of Carvalho *et al.* (2010) for its lack of prior tuning parameters and excellent shrinkage properties. Details on the non-centered parameterization, all prior specifications, posterior distributions and our sampling algorithm, alongside the extension to feature t-distributed errors are provided in Appendix A.

2.2. Dynamic sparsification

The model proposed above combined with continuous global-local shrinkage priors results in posterior draws that are pushed towards approximate sparsity. But the probability of observing exact zeroes remains zero. As a solution, we rely on ex post sparsification of the draws for each point in time. As highlighted by Hahn and Carvalho (2015), the success of the two-step shrink-then-sparsify approach depends on the shrinkage properties of the prior. They note that the horseshoe prior is well suited for such procedures, which is another reason why we illustrate our proposed framework with this specific choice.

To perform variable selection and obtain sparse coefficient matrices we post-process $\boldsymbol{\Pi}_t$, \mathbf{A}_t and $\boldsymbol{\Sigma}_t$ by minimizing three coefficient-type specific Lasso loss functions. In particular, we rely on methods proposed in Friedman *et al.* (2008), Hahn and Carvalho (2015), Chakraborty *et al.* (2020), Ray and Bhattacharya (2018), and Bashir *et al.* (2019), which have been successfully used in a range of multivariate and univariate macroeconomic and finance applications (see Puelz

et al., 2017; 2020; Huber *et al.*, 2020a; Hauzenberger *et al.*, 2020b). In cointegration models with time-varying parameters, however, it is necessary to adjust the proposed procedures for specific parts of the parameter space. Given the properties of the reduced-rank matrix $\mathbf{\Pi}_t$, we propose minor modifications when compared to sparsification of the autoregressive coefficients, \mathbf{A}_t , and the contemporaneous relations in the covariance matrix $\mathbf{\Sigma}_t$. Draws from the non-sparsified posteriors are indicated by a hat (e.g., $\hat{\mathbf{\Pi}}_t$), sparse estimates are denoted by an asterisk (e.g., $\mathbf{\Pi}_t^*$).

Sparsifying the cointegration matrix

Our basic approach to sparsifying the cointegration relationships follows Chakraborty *et al.* (2020). Ex post sparsifying $\mathbf{\Pi}_t$ is of crucial importance to obtain an estimate for the rank. Using only the shrinkage prior, some estimates in $\mathbf{\Pi}_t$ are pushed towards zero, but they are never exactly zero. This implies that $\mathbf{\Pi}_t$ would always be of full rank (i.e., $r = M$). The goal is to minimize the predictive loss between a draw $\hat{\mathbf{\Pi}}_t$ and a column-sparse solution $\mathbf{\Pi}_t^*$. Our interest centers on dynamic sparsification to obtain a sparse cointegration matrix at each point in time.

The loss function is specified in terms of the full-data matrix \mathbf{W} , a $T \times q$ matrix with \mathbf{w}'_t in the t th row:

$$\mathbf{\Pi}_t^{*'} = \arg \min_{\mathbf{\Pi}_t} \left(\|\mathbf{W}\hat{\mathbf{\Pi}}_t' - \mathbf{W}\mathbf{\Pi}_t'\|_F^2 + \sum_{j=1}^q \kappa_{jt} \|\mathbf{\Pi}_{\bullet,j,t}\|_2 \right), \quad (5)$$

with $\|\mathbf{C}\|_F$ denoting the Frobenius norm⁴ of a matrix \mathbf{C} , $\|\mathbf{c}\|_2$ the Euclidean norm of a vector \mathbf{c} and $\mathbf{\Pi}_{\bullet,j,t}$ referring to the j th column of $\mathbf{\Pi}_t$ (i.e., the j th row of its transpose). Equation (5) denotes a grouped Lasso problem with a row (column)-specific penalty κ_{jt} and aims at finding a row (column)-sparse solution of $\mathbf{\Pi}_t'$ ($\mathbf{\Pi}_t$).⁵ The first part controls the distance between an estimate and a sparse solution (measured by the Frobenius norm), while the second part penalizes non-zero elements in $\mathbf{\Pi}_t$ (in terms of column-specific Euclidean norms).

To avoid cross-validation for the penalty term (as in Hahn and Carvalho, 2015), we rely on the signal adaptive variable selection (SAVS) estimator proposed in Ray and Bhattacharya (2018) and set the penalty term to $\kappa_{jt} = 1/\|\hat{\mathbf{\Pi}}_{\bullet,j,t}\|_2^2$. This yields the following soft threshold estimate:⁶

$$\mathbf{\Pi}_{\bullet,j,t}^* = \begin{cases} \mathbf{0}_{M \times 1}, & \text{if } \frac{\kappa_{jt}}{2\|\hat{\mathbf{\Pi}}_{\bullet,j,t}\|_2} \geq \|\mathbf{W}_{\bullet,j}\|_2^2, \\ \left(1 - \frac{\kappa_{jt}}{2\|\mathbf{W}_{\bullet,j}\|_2^2\|\hat{\mathbf{\Pi}}_{\bullet,j,t}\|_2}\right) \hat{\mathbf{\Pi}}_{\bullet,j,t}, & \text{otherwise.} \end{cases} \quad (6)$$

⁴ The Frobenius norm is a common distance measure between subspaces and is given by $\|\mathbf{C}\|_F = \sqrt{\text{tr}(\mathbf{C}'\mathbf{C})}$ with $\text{tr}(\mathbf{C})$ denoting the trace of a matrix \mathbf{C} .

⁵ For a detailed discussion on properties of the grouped-lasso, see Yuan and Lin (2006) and Wang and Leng (2008).

⁶ To solve the optimization problem in Eq. (5), the SAVS estimator can be interpreted as special case of the coordinate descent algorithm (Friedman *et al.*, 2007) by relying on a single iteration to obtain a closed-form solution. Ray and Bhattacharya (2018) and Hauzenberger *et al.* (2020b) both provide evidence that the coordinate descent algorithm already converges after the first pass through.

As shown by Ray and Bhattacharya (2018) this choice of κ_{jt} has properties similar to the adaptive Lasso proposed by Zou (2006).

An estimate of the time-varying rank r_t after post-processing is

$$r_t = \sum_{i=1}^M \mathcal{I}(s_{it} > \varphi),$$

with $\mathcal{I}(\bullet)$ denoting the indicator function and s_{it} for $i = 1, \dots, M$ are the singular values of $\mathbf{W}\boldsymbol{\Pi}_t^{*'}.$ We follow Chakraborty *et al.* (2020) and define the rank as the number of non-thresholded singular values with φ defined as the largest singular value of the residuals of the full data specification of Eq. (1), corresponding to the maximum noise level.

So far, we remained silent on two crucial issues involved with dynamic sparsification. It is also worth noting that these issues are not specific to sparsification of $\boldsymbol{\Pi}_t$, but also relevant when sparsifying \mathbf{A}_t and $\boldsymbol{\Sigma}_t$ with respect to t :

1. Ex post sparsification is commonly applied to point estimators, such as the posterior median or mean. Eq. (5) can be interpreted as minimizing the expected loss (see Hahn and Carvalho, 2015). By following Huber *et al.* (2020a) and Hauzenberger *et al.* (2020b) we deviate from this procedure and solve the optimization problem for each draw from the posterior distribution. Setting $\hat{\boldsymbol{\Pi}}_t = \boldsymbol{\Pi}_t^{(s)}$ with (s) indicating the s th draw, has the convenient feature of effectively allowing for uncertainty quantification of the rank of $\boldsymbol{\Pi}_t$.⁷
2. Why does Eq. (5) feature the full-data matrix \mathbf{W} instead of the t -specific covariates \mathbf{w}_t' ? The latter might be considered as the natural candidate when transforming a TVP model to its static representation (for details, see Chan and Jeliazkov, 2009; Hauzenberger *et al.*, 2019). Commonly, sparsification is applied in standard regression framework with constant coefficients with the variation explained by $\mathbf{W}\boldsymbol{\Pi}'$. Using the static regression framework to perform dynamic sparsification and solely the t th observation \mathbf{w}_t' , instead of the full data matrix \mathbf{W} in Eq. (5), however, results in a serious problem due to dependency on a single observation in time t .

To illustrate this, we focus on the j th columns in both $\mathbf{W}_{\bullet j}$ and $\boldsymbol{\Pi}_{\bullet j}$. In the following, the norm of $\mathbf{W}_{\bullet j}$ is defined by $\|\mathbf{W}_{\bullet j}\|_2 = \sqrt{\sum_{t=1}^T w_{tj}^2}$. When using each observation and observation-specific estimate independently, the norm of the t th observation is given by $\|w_{tj}\|_2 = \sqrt{w_{tj}^2}$. The simplest approach would be to down-weight the penalty in Eq. (6) by a factor T . However, this approach, although theoretically in line with the sparsification techniques proposed in Hahn and Carvalho (2015), still has the disadvantage of being highly dependent on the t th observation. This is particularly problematic with seasonal data such as electricity prices. Therefore, using \mathbf{W} can be seen as practicable solution, where each t -specific estimate is used for the entire sample.⁸

⁷ Closely related to this approach is the procedure of Woody *et al.* (2020), who also provide a theoretical motivation of conducting uncertainty quantification of sparse posterior estimates.

⁸ The non-centered parameterization and random walk law of motion of the coefficients are in line with this strategy, since all information in \mathbf{W} is used to filter and smooth the time-varying parameters.

Regarding the SAVS algorithm, the only part that changes is how the norm of the data is calculated ($\|\mathbf{W}_{\bullet,j}\|_2^2$ instead of w_{jt}^2). In this case, the penalty specified in Chakraborty *et al.* (2020), $\kappa_{jt} = 1/(\|\hat{\mathbf{\Pi}}_{\bullet,j,t}\|_2^2)$, can be used (without correcting for T). Note that this is highly a practicable solution from an applied perspective, since the norm over the full data matrix is more robust than considering a single observation in period t .

Sparsifying the autoregressive coefficients

For sparsifying the time-varying autoregressive coefficients, we employ the methods proposed in Hahn and Carvalho (2015) and Ray and Bhattacharya (2018). We define a full-data matrix \mathbf{X} of dimension $T \times J$ with \mathbf{x}'_t in the t th row, an $MJ \times 1$ -vector $\mathbf{a}_t = \text{vec}(\mathbf{A}_t)$ and the corresponding regressor matrix $\tilde{\mathbf{X}} = (\mathbf{I}_M \otimes \mathbf{X})$ of dimension $T \times MJ$. We assume a loss function of the form:

$$\mathbf{a}_t^* = \arg \min_{\mathbf{a}_t} \left(\frac{1}{2} \|\tilde{\mathbf{X}} \hat{\mathbf{a}}_t - \tilde{\mathbf{X}} \mathbf{a}_t\|_2^2 + \sum_{j=1}^J \delta_{jt} |a_{jt}| \right), \quad (7)$$

with a_{jt} denoting the j th element of \mathbf{a}_t and δ_{jt} a covariate-specific penalty. It is worth noting that we minimize a standard Lasso-type predictive loss, different to the sparsification of the cointegration relationships, where the first part controls the distance between an estimate and a sparse solution and the second part penalizes non-zero elements in \mathbf{a}_t .

An optimal choice for the penalty is $\delta_{jt} = 1/(\hat{a}_{jt}^2)$. We again rely on the soft threshold estimate implied by SAVS to obtain a sparse draw of \mathbf{a}_t :

$$a_{jt}^* = \begin{cases} 0, & \text{if } \frac{\delta_{jt}}{|\hat{a}_{jt}|} \geq \|\tilde{\mathbf{X}}_{\bullet,j}\|_2^2, \\ \left(1 - \frac{\delta_{jt}}{\|\tilde{\mathbf{X}}_{\bullet,j}\|_2^2 |\hat{a}_{jt}|}\right) \hat{a}_{jt}, & \text{otherwise.} \end{cases} \quad (8)$$

As shown by Ray and Bhattacharya (2018) this choice of δ_{jt} again has properties similar to the adaptive Lasso proposed by Zou (2006).

Sparsifying the covariance matrix

A sparse draw of the covariance matrix can be obtained by relying on methods proposed in Friedman *et al.* (2007) and Bashir *et al.* (2019). Here, we post-process estimates of the precision matrix Σ_t^{-1} using the graphical Lasso:

$$\Sigma_t^{-1*} = \arg \min_{\Sigma_t^{-1}} \left(\text{tr} \left(\Sigma_t^{-1} \hat{\Sigma}_t \right) - \log \det \left(\Sigma_t^{-1} \right) + \sum_{i \neq j} \lambda_{ij,t} |\sigma_{ij,t}^{-1}| \right), \quad (9)$$

with $\text{tr}(\mathbf{C})$ and $\log \det(\mathbf{C})$ denoting the trace and the log-determinant of a square matrix \mathbf{C} and $\lambda_{ij,t}$ denotes an element-specific lasso penalty. Similar to Eq. (5) and Eq. (7) the parts $\text{tr} \left(\Sigma_t^{-1} \hat{\Sigma}_t \right) - \log \det \left(\Sigma_t^{-1} \right)$ are measures of fit, while the third term penalizes non-zero elements in the precision matrix. Here, it is worth noting that if $\sigma_{ij,t}^{-1*}$ is set to zero, the i th and the j th endogenous variable in the system do not feature a contemporaneous relationship.

Following Bashir *et al.* (2019), the penalty in Eq. (9) is chosen as $\lambda_{ij,t} = 1/|\sigma_{ij,t}^{-1}|^{0.5}$ with $\sigma_{ij,t}^{-1}$ denoting the j th element in the i th row of Σ_t^{-1} , which constitutes a semi-automatic procedure to circumvent cross-validation. Here, we refrain from showing the exact form of the soft threshold estimates for each element in Σ_t^{-1*} and refer to Friedman *et al.* (2008) instead, who define a set of soft threshold problems, similar to Eq. (8), to solve for an optimal solution for each element in Σ_t . We use the coordinate descent algorithm provided by Friedman *et al.* (2019) and only iterate once in line with the SAVS estimator.⁹

3. MODELING ELECTRICITY PRICES

We split our empirical application into two parts. First, we assess several in-sample features of the data using a set of countries and daily data. This serves to illustrate our approach in terms of detecting suitable cointegration relationships between interlinked energy markets across countries. Second, we conduct a detailed forecast evaluation, selecting Germany as the country of interest using hourly data. Here, we evaluate our approach against a large set of competing models. This exercise serves to showcase that the sparse TVP-VECM is capable of detecting sensible cointegration patterns in data (in this case, between hours during the day) when no prior knowledge of such relationships is available, and that it performs well for out-of-sample forecasts.

3.1. Data

For the first application, we use daily prices (in levels, averaged over the hours of the day) to estimate our model jointly for nine different regions/countries: Baltics (BALT), Denmark (DK), Finland (FI), France (FR), Germany (DE), Italy (IT), Norway (NO), Sweden (SE) and Switzerland (SI); i.e., $M = 9$. The data are available for the period from January 1st, 2017 to December 31st, 2019 in euros/MWh (megawatt-hour). We follow the literature and choose day-ahead prices determined on a specific day for delivery in a certain hour on the following day.

Prices for BALT and the Nordic countries (DK, FI, NO, SE) are obtained from *Nord Pool*; the German, Swiss and French hourly auction prices are from the power spot market of the *European Energy Exchange* (EEX); for the Italian prices, we use the single national prices (PUN) from the Italian system operator *Gestore dei Mercati Energetici* (GEM). We preprocess the data for daylight saving time changes to exclude the 25th hour in October and to interpolate the 24th hour in March. As additional exogenous factors, we consider daily prices for coal and fuel and interpolate missing values for weekends and holidays. In particular, we use the closing settlement prices for coal (LMCYSPT) and one month forward ICE UK natural gas prices (NATBGAS) due to their importance for the dynamic evolution of electricity prices

⁹ Alternatively, one could also regularize the precision matrix by writing Σ_t^{-1} as M -dimensional set of nodewise regressions by using the triangularization decomposition outlined by Meinshausen and Bühlmann (2006). Friedman *et al.* (2008) and Banerjee *et al.* (2008) have shown that this approach constitutes a special case of Eq. (9) with M independent Lasso problems.

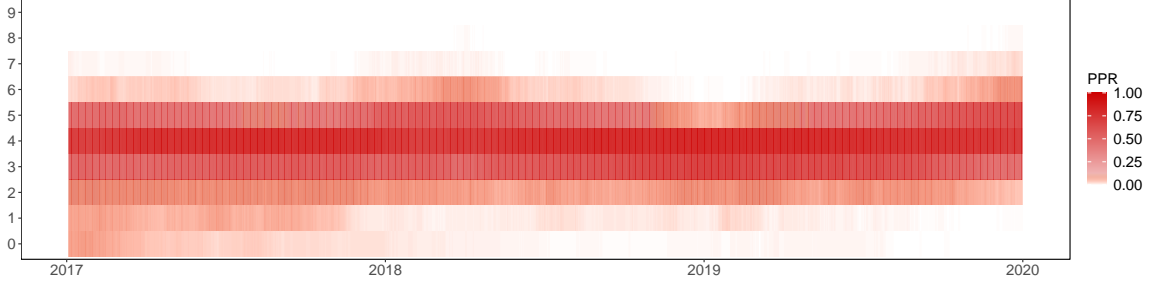


Fig. 1: Posterior probability of the rank (PPR) over time of the most flexible specification.

and potential cointegration relationships (i.e., $q = M + 2 = 11$). The model also features deterministic seasonal terms (encoded in \mathbf{c}_t) based on the respective day of the week.

In our second application, the forecast comparison, we choose hourly day-ahead prices (in levels) for Germany as our main country of interest, and focus on daylight hours (8 a.m. until 6 p.m.) and an average of the night hours (see also [Raviv et al., 2015](#)). We use a hold-out period of approximately a year and a half ranging from July 3rd, 2018 to December 31st, 2019 (in total 550 observations). We estimate TVP-VECMs with the individual hours per day being treated as dependent variables such that $M = 12$. Our exercise is based on a pseudo out-of-sample simulation using a rolling window of $T = 400$ observations at a time. We consider one-step ahead predictions, which implies that we forecast each individual hour for the following day. All models (both daily and hourly) feature $P = 2$ lags.

3.2. In-sample results for the cross-country analysis

We begin by illustrating one of the major novelties of our approach, that is, estimating a time-varying cointegration rank. Here, we compute the posterior probability of the rank (PPR) over time based on our MCMC output. The results are displayed in Figure 1, where probabilities are indicated in various shades of red. Several findings are worth noting. A rank larger than 9 is never supported, and while most posterior mass is concentrated on $r_t = 4$ for all t , we detect subtle differences over time.

At the beginning of the sample in 2017, our estimates are more dispersed, with non-negligible probabilities for no cointegration. The precision of our rank estimate increases over time, with a much narrower corridor of probabilities starting around 2018. After a brief period in late 2018 and early 2019 with probabilities shifting towards lower ranks, we find increases in cointegration relationships towards the end of the sample.

Next, we turn to sparsified estimates of the autoregressive coefficients and the error covariance matrix in panels (a) and (b) of Figure 2. Rather than showing magnitudes of the estimated coefficients, we use this exercise to illustrate the sparsification approach. As noted earlier, conventional shrinkage approaches push coefficients towards zero, but they are never exactly zero. The sparsification approach, on the other hand, introduces exact zeros in these matrices. We use this fact to compute the posterior inclusion probabilities (PIPs) of all coefficients by calculating the relative share of zeroes over the iterations of the algorithm. In other words, these figures showcase the sparsification approach as a variable selection tool (see [Hahn and Carvalho, 2015](#)).

We start with the coefficients linked to $\Delta \mathbf{y}_{t-p}$, that is, the dynamic interdependencies of the multivariate system in panel (a). A few findings are worth noting. First, we detect different degrees of sparsity across countries. While the Nordic and Baltic countries look rather similar (with comparatively dense coefficient matrices), this is not the case for Switzerland, Germany, Italy and France (CH, DE, FR and IT). For these countries, the model estimates rather sparse coefficient matrices. Second, the variables with the highest PIPs are typically the countries' own lagged series. Particularly France shows extremely sparse estimates, with non-zero inclusion probabilities only for its own lags. Third, we observe several interesting changes in PIPs over time. This implies changes in the importance of predictors over time, a feature which our model detects in a data-based fashion. Fourth, we observe some noteworthy patterns of dynamic interdependencies, namely between Nordic and Baltic countries on one side, and to a lesser degree between continental European economies.

A similar exercise of PIPs in the context of the sparse covariance matrix is displayed in panel (b). Here, we show the lower triangular part of the contemporaneous relationships over time. As in the case of the regression coefficients, we detect differences in the degree of sparsity over the cross-section and across time. Strong contemporaneous relationships are detected especially between the Nordic countries. The PIPs in this case are often exactly one, indicating that the respective coefficients feature non-zero draws across all iterations of the sampler. Similarly, albeit with lower inclusion probabilities, we find that covariances appear to be important between continental European electricity prices.

Interestingly, we observe a substantial degree of time-variation in the inclusion probabilities. Investigating these patterns in more detail, we find that the overall sparsity of the covariance matrix changes strongly over time, but does so in a specific way. In particular, there are periods where most covariance terms (apart from the always featured ones across Nordic countries) are sparsified strongly. Examples for such periods are in late 2017 and early 2018, or around the beginning of 2019. Again, it is noteworthy that our model discovers these features in an automatic fashion.

We complete our discussion of in-sample results by assessing whether heavy tailed errors are required to capture energy price fluctuations across the countries. For this purpose, we compare our estimates from our TVP-VECM benchmark model with stochastic volatility to the same specification with t-distributed errors (see Appendix A). The results for the parameters in the state equation of the time-varying error variances are displayed in Table 1.

A crucial parameter in the context of heavy tailed errors is ν_i , the degrees of freedom in the t-distribution. Note that as $\nu_i \rightarrow \infty$, this distribution approaches a Gaussian. Consequently, large estimates imply that Gaussian errors are sufficient for capturing large swings in energy prices. For most countries, estimates center around 15, resulting in an error distribution that looks almost like a Gaussian distribution, albeit with a bit heavier tails. This implies that information in our dataset suggests that t-distributed errors are no crucial feature for Baltic countries ($\nu = 13$), Switzerland ($\nu = 14$), Germany ($\nu = 16$), France ($\nu = 16$), Italy ($\nu = 17$) and Norway ($\nu = 15$). Differences appear for Denmark ($\nu = 7$), Finland ($\nu = 2$) and Sweden ($\nu = 4$), that are the nordic countries, apart from the case of Norway. Here, we observe degrees

of freedom between 2 and 7, with a substantial number of observations in the tails of the error distribution.

Turning to estimates of the unconditional mean, persistence and errors of the state equation, we find that for the countries exhibiting less need for heavy tails indicated by high estimates of ν_i , the posterior moments in Table 1, are almost identical. This is due to the more flexible error distribution approaching Gaussianity. For the nordic countries apart from Norway, we detect a pattern in terms of differences between parameter estimates. We observe substantially more persistent volatility processes for the heavy tailed specification, with lower variances for Denmark, Finland and Sweden. Differences in the unconditional mean are muted.

Next, we assess the log-volatilities over time and across countries. Figure 3 shows our estimates for t-distributed errors in panel (a), while panel (b) indicates the standard SV specification. A few things are worth noting here. First, while the level of the volatilities varies substantially over the cross-section (as indicated in the context of the unconditional mean in Table 1), the volatilities exhibit a substantial degree of co-movement. Second, even though we detect several differences between heavy tailed errors and conventional SVs, the first principal component of all volatility processes (marked by the red line) is almost identical for both error specifications. Third, t-distributed errors result in numerous high-frequency spikes for the nordic countries apart from Norway.

Summing up our discussion of required features of the error distribution, our results across countries are mixed. There is overwhelming empirical evidence for time-varying variances. Heavy tailed errors, on the other hand, are supported only for a subset of countries, namely Denmark, Finland and Sweden.

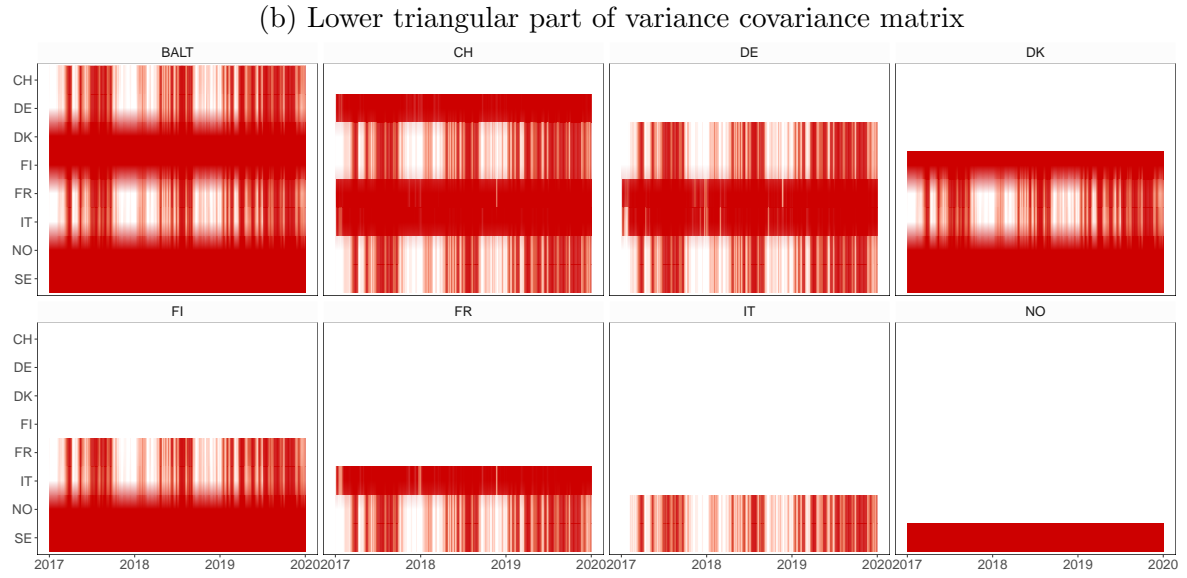
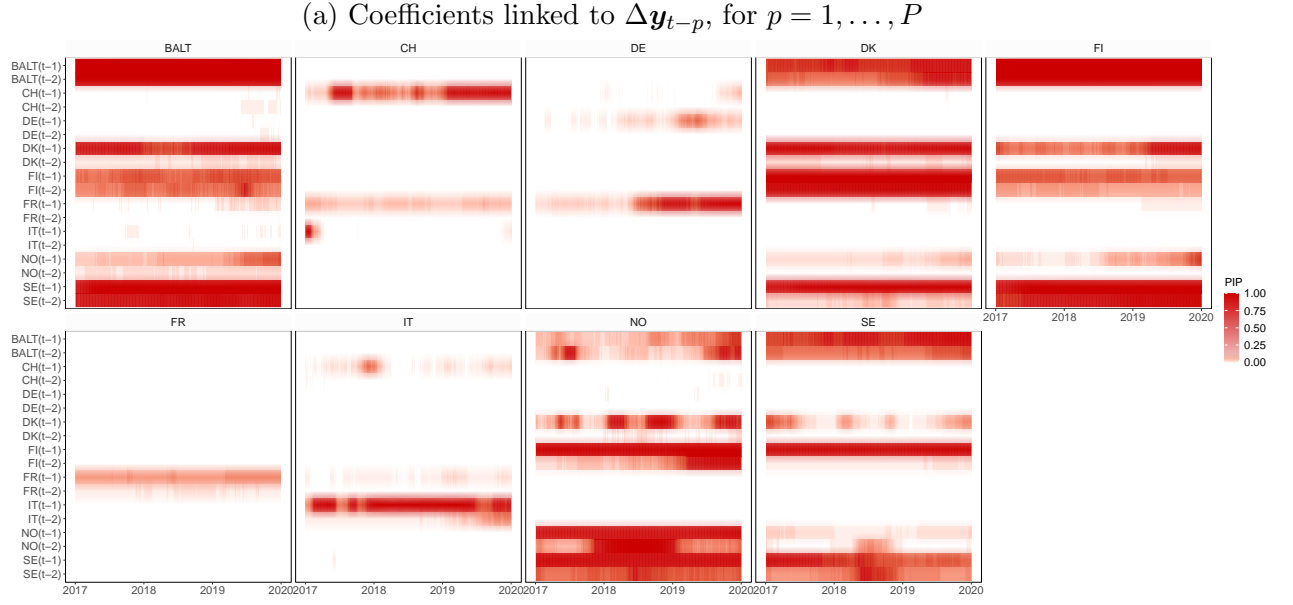


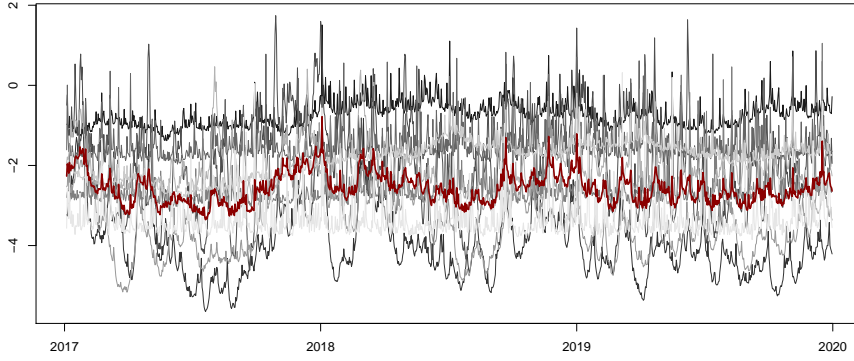
Fig. 2: Posterior inclusion probability (PIP) over time of autoregressive coefficients (panel (a)) and covariance matrices (panel (b)) of the most flexible specification.

Table 1: Posterior estimates for the state equations of the error variances.

t-distributed errors									
	<i>BALT</i>	<i>CH</i>	<i>DE</i>	<i>DK</i>	<i>FI</i>	<i>FR</i>	<i>IT</i>	<i>NO</i>	<i>SE</i>
μ_i	-0.584 (-0.835,-0.342)	-3.971 (-4.264,-3.7)	-1.782 (-2.066,-1.52)	-1.581 (-2.052,-1.19)	-3.688 (-4.068,-3.298)	-3.496 (-3.802,-3.218)	-2.139 (-2.327,-1.974)	-1.687 (-1.937,-1.435)	-3.635 (-4.194,-3.263)
ϕ_i	0.963 (0.93,0.987)	0.908 (0.866,0.942)	0.827 (0.766,0.883)	0.654 (0.362,0.873)	0.92 (0.759,0.977)	0.919 (0.885,0.947)	0.862 (0.809,0.91)	0.972 (0.937,0.992)	0.629 (0.401,0.783)
ς_i^2	0.125 (0.068,0.189)	0.459 (0.364,0.574)	0.742 (0.609,0.875)	0.364 (0.042,0.718)	0.17 (0.1,0.309)	0.431 (0.346,0.535)	0.398 (0.313,0.474)	0.103 (0.05,0.183)	0.595 (0.322,0.806)
ν_i	13.022 (8.316,18.307)	13.691 (7.015,19.346)	15.745 (9.796,19.612)	6.872 (2.822,15.421)	2.211 (2.012,2.574)	16.218 (11.11,19.69)	17.008 (12.837,19.849)	14.497 (8.966,19.589)	4.417 (2.276,7.675)
Gaussian errors									
	<i>BALT</i>	<i>CH</i>	<i>DE</i>	<i>DK</i>	<i>FI</i>	<i>FR</i>	<i>IT</i>	<i>NO</i>	<i>SE</i>
μ_i	-0.522 (-0.700,-0.330)	-3.903 (-4.165,-3.627)	-1.786 (-2.039,-1.534)	-1.655 (-1.787,-1.525)	-3.130 (-3.506,-2.771)	-3.572 (-3.839,-3.291)	-2.123 (-2.279,-1.952)	-1.650 (-1.864,-1.416)	-3.684 (-3.875,-3.407)
ϕ_i	0.924 (0.825,0.981)	0.876 (0.816,0.924)	0.807 (0.749,0.864)	0.238 (0.073,0.382)	0.346 (0.211,0.466)	0.893 (0.843,0.932)	0.826 (0.765,0.882)	0.938 (0.796,0.988)	0.309 (0.184,0.428)
ς_i^2	0.202 (0.092,0.351)	0.560 (0.436,0.720)	0.817 (0.682,0.961)	1.016 (0.905,1.143)	1.220 (1.006,1.489)	0.508 (0.404,0.633)	0.473 (0.381,0.578)	0.172 (0.07,0.391)	1.227 (1.047,1.386)

Notes: The parameter ν_i are the degrees of freedom for the t-distribution. If $\nu_i \rightarrow \infty$, the errors approach a Gaussian distribution. μ_i denotes the unconditional mean, ϕ_i the autoregressive parameter, and ς_i^2 the state variances of the M independent latent log-volatility processes h_{it} . Posterior median alongside 90% credible sets in parentheses.

(a) Stochastic volatility with t-distributed errors:



(b) Stochastic volatility with Gaussian-distributed errors

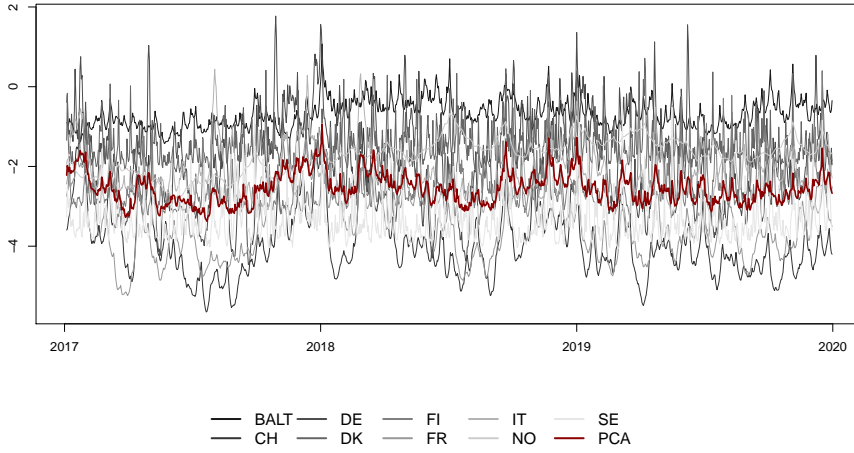


Fig. 3: Posterior median of stochastic volatility. The red line denotes the first principal component (PCA) of M latent processes (h_{it}).

3.3. Forecast results

In our forecasting comparison, we zoom in on a single country to conduct a thorough analysis featuring many competing models that have been shown to work well in the previous literature. In particular, we select hourly day-ahead prices for Germany, and evaluate point and density forecasts for a set of models that are described in detail below.

Competing models

The competing specifications are a large set of univariate and multivariate models with constant and time-varying parameters. Moreover, we consider several choices for including heteroscedastic errors. The full set of models is the following:

- *Model variants:* As simple univariate competitors, we use $AR(P)$ models in levels (**ARp1**) and differences (**ARpd**, this model serves as the benchmark). The set of multivariate models is

given by vector autoregressions (VARs) in levels (VARl) and differences (VARd), and vector error correction models (VECM) with a fixed rank $\bar{r} \in \{2, 4\}$.

- *Autoregressive parameters*: All models are estimated with time-invariant (TIV) and time-varying (TVP) parameters.
- *Stochastic disturbances*: We consider heteroscedasticity by either relying on a conventional stochastic volatility specification with Gaussian errors (iSV-n) as in Eq. (4), or an extension with t-distributed errors (iSV-t) described in Appendix A.

Recall that all models feature two lags, i.e., two full days worth of hourly lags ($P = 2$) and are equipped with a horseshoe prior (Carvalho *et al.*, 2010), see Appendix A for details. We refrain from showing results for homoscedastic specifications, since these models are typically found to be inferior for forecasting (see, for instance, Gianfreda *et al.*, 2020).

Point and density forecasts

We assess the forecast performance for the first and second moments of the predictive distribution for electricity prices in Germany. Root mean squared errors (RMSEs) serve to evaluate the point predictions across our models. As a measure capturing density forecast performance, we rely on the continuous ranked probability score (CRPS). We choose CRPSs rather than log predictive scores, since they are less sensitive to outliers and superior in rewarding predictive densities that are close to but not exactly equal to outcomes (see Gneiting and Raftery, 2007; Gneiting and Ranjan, 2011).¹⁰

Table 2 displays RMSEs and CRPSs across all model types (rows) and over the respective hours of the day (columns). Forecasts are produced hourly for a full-day (8 a.m. until 6 p.m., and aggregate “Night” hours). Besides individual hours, we produce a summary figure for overall forecast performance across a full day (labeled “Total”). Model abbreviations and variants of features such as TVPs or the error variances specification are indicated in the previous Subsection. Values in the first row per model indicate RMSEs, those in parentheses in the second row are CRPSs. They are benchmarked relative (as ratios) to the AR(P) model in differences with constant parameters and a standard stochastic volatility specification (ARpd, red shaded row, indicating actual values of RMSEs and CRPSs). In both cases, small relative numbers mark superior forecast performance, with the best performing specification in bold.

The upper panel contains results for our main specification with sparsified estimates. The lower panel shows several non-sparsified benchmarks. It is worth mentioning that many of these benchmark specifications are nested in our proposed model. Examples would be specifications with fixed cointegration rank, or VARs in levels (in the case where our approach selects the cointegration matrix to be of full rank). Such specifications in essence differ only in terms of the implied prior on the reduced form coefficients (see, for instance, Villani, 2009; Eisenstat *et al.*, 2016; Giannone *et al.*, 2019).

¹⁰Log predictive scores are available from the corresponding author upon request.

Table 2: Forecast performance for point and density forecasts in parentheses relative to the benchmark.

Specification			1-day-ahead												
Class	TVP	SV	Total	8 a.m.	9 a.m.	10 a.m.	11 a.m.	12 a.m.	1 p.m.	2 p.m.	3 p.m.	4 p.m.	5 p.m.	6 p.m.	Night
Main (sparsified)															
VECM	TVP	t	0.78 (0.44)	0.80 (0.71)	0.79 (0.72)	0.79 (0.78)	0.79 (0.79)	0.82 (0.82)	0.83 (0.85)	0.82 (0.85)	0.82 (0.84)	0.84 (0.84)	0.86 (0.85)	0.91 (0.92)	0.91 (0.94)
VECM	TVP	n	0.78 (0.42)	0.80 (0.68)	0.78 (0.69)	0.78 (0.73)	0.78 (0.74)	0.81 (0.78)	0.83 (0.80)	0.83 (0.79)	0.82 (0.78)	0.84 (0.80)	0.86 (0.82)	0.91 (0.88)	0.91 (0.87)
VECM	TIV	t	0.78 (0.44)	0.80 (0.70)	0.78 (0.70)	0.78 (0.77)	0.78 (0.80)	0.81 (0.85)	0.83 (0.86)	0.82 (0.87)	0.82 (0.86)	0.85 (0.88)	0.87 (0.88)	0.93 (0.85)	0.91 (0.87)
VECM	TIV	n	0.76 (0.44)	0.79 (0.70)	0.77 (0.71)	0.76 (0.76)	0.79 (0.79)	0.82 (0.84)	0.81 (0.85)	0.81 (0.86)	0.81 (0.85)	0.84 (0.86)	0.85 (0.87)	0.91 (0.84)	0.89 (0.87)
Benchmarks (non-sparsified)															
VECM	TVP	t	0.75 (0.44)	0.76 (0.71)	0.75 (0.72)	0.75 (0.78)	0.76 (0.79)	0.79 (0.83)	0.82 (0.85)	0.80 (0.85)	0.79 (0.84)	0.82 (0.84)	0.84 (0.85)	0.90 (0.91)	0.90 (0.93)
VECM	TVP	n	0.76 (0.44)	0.76 (0.75)	0.75 (0.75)	0.75 (0.78)	0.76 (0.78)	0.79 (0.82)	0.82 (0.82)	0.81 (0.83)	0.80 (0.83)	0.85 (0.84)	0.85 (0.86)	0.90 (0.90)	0.90 (0.92)
VECM - 2	TVP	n	0.74 (0.43)	0.76 (0.70)	0.74 (0.71)	0.75 (0.76)	0.77 (0.77)	0.79 (0.81)	0.81 (0.83)	0.81 (0.82)	0.79 (0.81)	0.81 (0.83)	0.83 (0.85)	0.84 (0.89)	0.88 (0.92)
VECM - 4	TVP	n	0.74 (0.42)	0.75 (0.69)	0.74 (0.69)	0.75 (0.75)	0.77 (0.77)	0.79 (0.79)	0.80 (0.81)	0.80 (0.82)	0.78 (0.80)	0.80 (0.82)	0.83 (0.84)	0.84 (0.82)	0.88 (0.88)
VECM	TIV	t	0.75 (0.42)	0.75 (0.69)	0.75 (0.69)	0.75 (0.75)	0.76 (0.76)	0.79 (0.78)	0.82 (0.80)	0.80 (0.81)	0.79 (0.79)	0.83 (0.81)	0.85 (0.82)	0.91 (0.82)	0.90 (0.87)
VECM	TIV	n	0.75 (0.44)	0.75 (0.74)	0.74 (0.75)	0.74 (0.76)	0.75 (0.77)	0.78 (0.80)	0.82 (0.81)	0.80 (0.82)	0.80 (0.82)	0.82 (0.84)	0.85 (0.86)	0.90 (0.89)	0.88 (0.92)
VECM - 2	TIV	n	0.74 (0.44)	0.75 (0.75)	0.74 (0.76)	0.75 (0.77)	0.77 (0.78)	0.79 (0.81)	0.81 (0.81)	0.81 (0.82)	0.79 (0.82)	0.81 (0.84)	0.83 (0.87)	0.84 (0.92)	0.88 (0.93)
VECM - 4	TIV	n	0.74 (0.42)	0.76 (0.69)	0.75 (0.69)	0.76 (0.75)	0.77 (0.77)	0.79 (0.79)	0.80 (0.81)	0.80 (0.82)	0.78 (0.80)	0.81 (0.82)	0.83 (0.83)	0.84 (0.82)	0.88 (0.87)
VARl	TVP	t	0.77 (0.42)	0.76 (0.69)	0.76 (0.69)	0.77 (0.75)	0.79 (0.76)	0.82 (0.78)	0.83 (0.80)	0.82 (0.81)	0.81 (0.79)	0.84 (0.81)	0.87 (0.82)	0.87 (0.82)	0.90 (0.87)
VARl	TVP	n	0.77 (0.42)	0.77 (0.71)	0.77 (0.72)	0.78 (0.73)	0.80 (0.73)	0.83 (0.77)	0.84 (0.77)	0.83 (0.78)	0.82 (0.79)	0.85 (0.81)	0.88 (0.83)	0.88 (0.87)	0.90 (0.87)
VARl	TIV	t	0.75 (0.46)	0.75 (0.72)	0.74 (0.73)	0.76 (0.80)	0.78 (0.83)	0.81 (0.89)	0.81 (0.90)	0.81 (0.91)	0.79 (0.90)	0.82 (0.92)	0.85 (0.93)	0.85 (0.90)	0.87 (0.93)
VARl	TIV	n	0.76 (0.46)	0.76 (0.73)	0.75 (0.73)	0.77 (0.80)	0.79 (0.83)	0.82 (0.88)	0.82 (0.88)	0.82 (0.89)	0.80 (0.88)	0.83 (0.91)	0.86 (0.92)	0.85 (0.90)	0.88 (0.93)
VARd	TVP	n	0.91 (0.54)	0.94 (0.89)	0.94 (0.89)	0.94 (0.97)	0.95 (0.98)	0.96 (1.02)	0.96 (1.01)	0.97 (1.04)	0.99 (1.03)	0.99 (1.06)	1.00 (1.05)	0.98 (1.00)	0.99 (1.00)
VARd	TIV	t	0.89 (0.53)	0.92 (0.88)	0.92 (0.88)	0.93 (0.97)	0.94 (0.98)	0.95 (1.02)	0.95 (1.01)	0.95 (1.03)	0.94 (1.02)	0.97 (1.05)	0.99 (1.05)	0.96 (1.00)	0.98 (0.99)
VARd	TIV	n	0.91 (0.56)	0.94 (0.92)	0.94 (0.93)	0.94 (1.02)	0.95 (1.03)	0.97 (1.08)	0.97 (1.07)	0.97 (1.08)	0.96 (1.07)	0.99 (1.10)	1.00 (1.09)	0.98 (1.05)	1.00 (1.06)
ARpl	TVP	n	0.81 (0.44)	0.84 (0.78)	0.82 (0.78)	0.84 (0.79)	0.86 (0.81)	0.86 (0.82)	0.86 (0.82)	0.87 (0.84)	0.86 (0.83)	0.88 (0.84)	0.90 (0.85)	0.87 (0.83)	0.92 (0.89)
ARpl	TIV	t	0.83 (0.46)	0.89 (0.85)	0.87 (0.83)	0.88 (0.83)	0.87 (0.83)	0.86 (0.83)	0.88 (0.84)	0.87 (0.84)	0.86 (0.83)	0.89 (0.85)	0.91 (0.87)	0.88 (0.84)	0.92 (0.90)
ARpl	TIV	n	0.86 (0.49)	0.91 (0.90)	0.89 (0.88)	0.91 (0.90)	0.90 (0.89)	0.89 (0.90)	0.91 (0.91)	0.90 (0.91)	0.89 (0.90)	0.89 (0.93)	0.94 (0.94)	0.92 (0.92)	0.97 (1.00)
ARpd	TVP	n	0.94 (0.54)	1.00 (1.00)	1.01 (1.01)	1.00 (1.00)	1.00 (1.00)	1.00 (1.00)	0.99 (0.99)	1.00 (1.00)	1.00 (1.00)	1.01 (1.00)	0.99 (0.99)	0.99 (0.99)	1.00 (1.01)
ARpd	TIV	t	0.93 (0.52)	0.99 (0.98)	0.99 (0.97)	0.99 (0.98)	1.00 (0.97)	0.98 (0.96)	0.99 (0.97)	0.99 (0.97)	0.98 (0.96)	1.00 (0.97)	0.99 (0.97)	0.98 (0.96)	0.98 (0.95)
ARpd	TIV	n	0.94 (0.54)	1.09 (0.68)	1.03 (0.62)	0.99 (0.58)	0.98 (0.57)	0.94 (0.54)	0.95 (0.55)	0.96 (0.54)	0.96 (0.55)	0.90 (0.52)	0.88 (0.50)	0.85 (0.49)	0.69 (0.37)

Notes: Point forecasts are evaluated using root mean squared errors (RMSEs), density forecasts are continuous ranked probability scores (CRPS). The red shaded rows denote the benchmark and displays actual values for RMSEs and CRPSs. All other models are shown as ratios to the benchmark.

Our results indicate the lack of a single best performing specification. While almost all multivariate models are superior compared to the univariate benchmarks, we obtain mixed evidence on whether one should choose VAR or VECM specifications for forecasting electricity prices. Relatedly, no clear picture emerges on the necessity of heavy tailed error distributions. The latter finding is in line with our discussion of in-sample findings for Germany in Section 3.2. Here, we found that when estimating a model with t-distributed errors, the large estimates for the degrees of freedom parameter suggests that a Gaussian error distribution is sufficient. It is worth mentioning, however, that t-distributed errors never substantially hurt predictive performance. In sum, we find that all of our multivariate competing models, sparsified and non-sparsified, exhibit similar performance. In what follows, we describe our findings for point and density forecasts in more detail.

Starting with point forecasts, Table 2 indicates the non-sparsified TVP-VECM with Gaussian errors as the best performing specification. As suggested earlier, several other specifications, including our proposed model, display similar performance. These models show improvements upon the univariate benchmark model of about 20 to 25 percent lower RMSEs in magnitude. We find several interesting patterns throughout the hours of the day. While before noon the non-sparsified VECM with constant parameters and Gaussian errors performs best (albeit at small margins), we observe slightly larger relative RMSEs in the afternoon, with the TVP-VECM of rank $\bar{r} = 4$ showing the most promising metrics. For night hours, improvements for point forecasts relative to the simple univariate benchmark are muted.

Turning to density forecasts in terms of CRPSs, we observe several differences compared to point forecast performance orderings. While most models show substantial improvements between 50 to 60 percent lower CRPSs compared to the constant parameter AR_{pd} with conventional stochastic volatilities, this metric selects our proposed model with Gaussian errors as the best performing specification for the full day (see column “Total”). Note, however, that several of the multivariate benchmarks exhibit similar performance measures. It is also worth mentioning that relative CRPSs for the variant of our proposed model with t-distributed errors are only 2 percentage points larger, indicating that allowing for heavy tailed errors is not necessary for Germany, but also does not hurt density forecasts. This finding again corroborates our results discussed in the context of Sub-section 3.2. As was the case for point forecasts, we observe differences over the hours of the day. Our proposed model shows superior performance especially early in the morning and late in the afternoon, while the TVP-VAR in levels with Gaussian errors is favoured in the hours between. Similar as was the case for point forecasts, however, differences between models (apart from the univariate benchmarks) often seem negligible.

To gauge the significance of our results, we conduct a more thorough analysis of uncertainty surrounding our forecast metrics. Here, we employ the model confidence set (MCS) procedure of Hansen *et al.* (2011). For point forecasts, the loss function is specified in terms of mean squared errors, while for density forecasts it is specified in terms of CRPSs. Empty cells indicate that the corresponding model is eliminated from the MCS for the respective variable and loss function. The resulting MCS is displayed in Table 3.

Table 3: Model confidence set (MCS) for point and density forecasts.

Specification			1-day-ahead													
Class	TVP	SV	Tot.	h8	h9	h10	h11	h12	h13	h14	h15	h16	h17	h18	night	
Main (sparsified)																
VECM	TVP	t	16 (7)	(16)	(15)	16 (7)	14 (6)	16 (8)	14 (4)	14 (6)	15 (5)	5 (5)	7 (9)	(12)	14 (10)	
VECM	TVP	n	11 (5)	(15)	(16)	15 (4)	6 (2)	10 (3)	11 (2)	13 (4)	13 (6)	13 (8)	11 (10)	(10)	15 (8)	
VECM	TIV	t	14 (8)	(14)	12 (13)	14 (5)	11 (5)	14 (6)	8 (3)	11 (5)	12 (7)	9 (7)	6 (8)	(11)	13 (11)	
VECM	TIV	n	12 (2)	(13)	(14)	13 (1)	5 (1)	9 (1)	7 (1)	8 (1)	10 (2)	11 (2)	8 (4)	(17)	8 (3)	
Benchmarks (non-sparsified)																
VECM	TVP	t	3 (6)	4 (3)	5 (4)	3 (6)	4 (8)	2 (9)	2 (7)	1 (7)	3 (9)	3 (9)	4 (6)	(15)	9 (14)	
VECM	TVP	n	7 (4)	7 (2)	6 (3)	4 (3)	3 (3)	4 (4)	9 (5)	7 (3)	6 (3)	8 (4)	10 (5)	(14)	10 (9)	
VECM - 2	TVP	n	13 (15)	9 (12)	8 (5)	7 (10)	10 (15)	8 (13)	15 (17)	15 (16)	14 (15)	12 (15)	14 (17)	5 (7)	12 (22)	
VECM - 4	TVP	n	1 (3)	6 (7)	10 (7)	9 (9)	13 (11)	5 (5)	1 (9)	3 (10)	1 (4)	1 (3)	1 (3)	2 (1)	3 (1)	
VECM	TIV	t	4 (9)	3 (4)	4 (6)	2 (8)	2 (7)	3 (10)	3 (13)	2 (8)	2 (10)	4 (10)	5 (7)	(16)	6 (15)	
VECM	TIV	n	6 (1)	2 (1)	3 (2)	1 (2)	1 (4)	1 (2)	6 (6)	4 (2)	7 (1)	15 (1)	9 (1)	(18)	5 (6)	
VECM - 2	TIV	n	2 (12)	5 (10)	1 (1)	5 (11)	8 (14)	7 (14)	12 (16)	10 (15)	5 (16)	2 (13)	2 (12)	1 (5)	2 (18)	
VECM - 4	TIV	n	9 (10)	11 (9)	11 (10)	11 (12)	15 (12)	6 (7)	4 (10)	5 (11)	9 (8)	6 (6)	3 (2)	3 (2)	4 (5)	
VARl	TVP	t	8 (13)	8 (5)	7 (8)	6 (14)	7 (13)	11 (16)	10 (14)	9 (17)	8 (17)	10 (16)	13 (16)	(8)	7 (12)	
VARl	TVP	n	10 (11)	10 (6)	9 (9)	12 (13)	12 (9)	13 (15)	13 (12)	12 (14)	11 (14)	14 (17)	15 (14)	(6)	11 (13)	
VARl	TIV	t	5 (18)	1 (8)	2 (11)	8 (17)	9 (18)	12 (15)	5 (6)	6 (4)	4 (7)	7 (19)	12 (19)	4 (19)	1 (4)	
VARl	TIV	n	15 (17)	12 (11)	13 (12)	10 (16)	16 (17)	15 (18)	16 (18)	16 (18)	16 (18)	16 (18)	16 (18)	(13)	16 (2)	
VARd	TVP	n														
VARd	TIV	t														
VARd	TIV	n														
(20)																
ARpl	TVP	n	(16)				(15)	(16)	(11)	(11)	(13)	(11)	(11)	(11)	(3)	19 (7)
ARpl	TIV	t				(15)				(17)	(15)	(12)	(13)	(15)	(4)	18 (17)
ARpl	TIV	n				(14)	(10)			(12)	(8)	(9)	(12)	(13)	(9)	17 (16)
ARpd	TVP	n														
ARpd	TIV	t														
ARpd	TIV	n														
(21)																
(23)																
(19)																

Notes: Results for the model confidence set (MCS) procedure of Hansen *et al.* (2011) at a 25 percent significance level. The loss function is specified in terms of mean squared errors (MSEs, rank in first row per model) and CRPSs (rank in second row in parenthesis). Empty cells indicate that the model is **not** part of the MCS. The top three ranked models are marked in bold.

The MCS procedure yields a set of specifications which is a collection of models that contains the best ones with our pre-defined level of 75 percent confidence. Given the informativeness of the data, this procedure may either select a single best performing specification, or a ranking of several comparable models on our chosen level of 25 percent significance (see Hansen *et al.*, 2011). Considering the results of this exercise in Table 3, we find that our proposed model performs well overall, and that it is included in the MCS (i.e., not outperformed in terms of statistical significance) for both point and density forecasts in most hours.

However, we observe several differences when compared to our previous discussion of RMSEs and CRPSs. First, while our proposed model is included in the MCS for point and density forecasts in terms of overall forecast performance, this is not the case for several hours during the day in terms of point forecasts. Second, the MCS procedure yields a different performance ranking when compared to evaluating solely RMSEs and CRPSs and producing a ranking in absolute terms. We conjecture that this is due to several periods in our holdout sample that affect the end-of-sample metrics shown in Table 2, whereas the MCS procedure is more robust to such idiosyncrasies. Third, while our proposed model occupies mostly lower ranks for point forecasts, we observe high ranks particularly during the afternoon in terms of density forecasts. Finally, it is worth mentioning that VECMs generally appear to yield superior forecasts to VARs.

4. CONCLUDING REMARKS

In this paper, we propose a TVP-VECM with heteroscedastic errors equipped with shrinkage priors and discuss methods for inducing sparsity. This framework is capable of introducing exact zeroes in cointegration relationships, autoregressive coefficients and the covariance matrix. Moreover, our procedure yields estimates for a time-varying cointegration rank, without the need for introducing prior information on the cointegration relationships.

We estimate our model using daily and hourly day-ahead prices for different European electricity markets. In the empirical section, we illustrate some features of our approach within-sample, and conduct an extensive out-of-sample forecast comparison. Regarding the in-sample analysis, we detect several interesting time-varying patterns of sparsity in the autoregressive coefficients and the covariance matrix. We find that our approach is competitive for forecasting hourly day-ahead electricity prices when compared to a large set of univariate and multivariate benchmarks, featuring both time-varying parameters and heavy tailed error distributions.

REFERENCES

- BANERJEE O, GHAOUI LE, AND D’ASPREMONT A (2008), “Model selection through sparse maximum likelihood estimation for multivariate Gaussian or binary data,” *Journal of Machine Learning Research* **9**(Mar), 485–516.
- BASHIR A, CARVALHO CM, HAHN PR, AND JONES MB (2019), “Post-Processing Posteriors Over Precision Matrices to Produce Sparse Graph Estimates,” *Bayesian Analysis* **14**(4), 1075–1090.
- BELLO A, AND RENESES J (2013), “Electricity Price Forecasting in the Spanish Market using Cointegration Techniques,” in “The 33rd Annual International Symposium on Forecasting (ISF 2013) Forecasting with Big Data,” .
- BOSCO B, PARISIO L, PELAGATTI M, AND BALDI F (2010), “Long-Run Relations in European Electricity Prices,” *Journal of Applied Econometrics* **25**, 805–832.

- BUNEA F, SHE Y, AND WEGKAMP MH (2012), “Joint variable and rank selection for parsimonious estimation of high-dimensional matrices,” *The Annals of Statistics* **40**(5), 2359–2388.
- CARRIERO A, CLARK TE, AND MARCELLINO M (2019), “Large Bayesian vector autoregressions with stochastic volatility and non-conjugate priors,” *Journal of Econometrics* **212**(1), 137–154.
- CARTER C, AND KOHN R (1994), “On Gibbs sampling for state space models,” *Biometrika* **81**(3), 541–553.
- CARVALHO CM, POLSON NG, AND SCOTT JG (2010), “The horseshoe estimator for sparse signals,” *Biometrika* **97**(2), 465–480.
- CHAKRABORTY A, BHATTACHARYA A, AND MALICK BK (2020), “Bayesian sparse multiple regression for simultaneous rank reduction and variable selection,” *Biometrika* **107**(1), 205–221.
- CHAN JC, AND JELIAZKOV I (2009), “Efficient simulation and integrated likelihood estimation in state space models,” *International Journal of Mathematical Modelling and Numerical Optimisation* **1**(1-2), 101–120.
- CHUA CL, AND TSIAPLIAS S (2018), “A Bayesian Approach to Modeling Time-Varying Cointegration and Cointegrating Rank,” *Journal of Business & Economic Statistics* **36**(2), 267–277.
- DE MARCOS RA, RENESES J, AND BELLO A (2016), “Long Term Spanish Electricity Market Price Forecasting with Cointegration and VEC Models,” in “International Conference on Probabilistic Methods Applied to Power Systems (PMAPS),” .
- DE VANY A, AND WALLS W (1999), “Cointegration analysis of spot electricity prices: insights on transmission efficiency in the western US,” *Energy Economics* **21**(5), 435–448.
- EISENSTAT E, CHAN JC, AND STRACHAN RW (2016), “Stochastic model specification search for time-varying parameter VARs,” *Econometric Reviews* **35**(8-10), 1638–1665.
- FRIEDMAN J, HASTIE T, HÖFLING H, TIBSHIRANI R, *et al.* (2007), “Pathwise coordinate optimization,” *The Annals of Applied Statistics* **1**(2), 302–332.
- FRIEDMAN J, HASTIE T, AND TIBSHIRANI R (2008), “Sparse inverse covariance estimation with the graphical lasso,” *Biostatistics* **9**(3), 432–441.
- (2019), *glasso: Graphical Lasso: Estimation of Gaussian Graphical Models*, R package version 1.11.
- FRÜHWIRTH-SCHNATTER S (1994), “Data augmentation and dynamic linear models,” *Journal of Time Series Analysis* **15**(2), 183–202.
- FRÜHWIRTH-SCHNATTER S, AND WAGNER H (2010), “Stochastic model specification search for Gaussian and partial non-Gaussian state space models,” *Journal of Econometrics* **154**(1), 85–100.
- GEWEKE J (1996), “Bayesian reduced rank regression in econometrics,” *Journal of Econometrics* **75**(1), 121–146.
- GIANFREDA A, PARISIO L, AND PELAGATTI M (2019), “The RES-Induced Switching Effect Across Fossil Fuels: An Analysis of Day-Ahead and Balancing Prices,” *The Energy Journal* **40**.
- GIANFREDA A, RAVAZZOLO F, AND ROSSINI L (2020), “Large time-varying volatility models for electricity prices,” *CAMP BI Working Paper 05/2020* .
- GIANNONE D, LENZA M, AND PRIMICERI GE (2019), “Priors for the long run,” *Journal of the American Statistical Association* **114**(526), 565–580.
- GNEITING T, AND RAFTERY AE (2007), “Strictly proper scoring rules, prediction, and estimation,” *Journal of the American statistical Association* **102**(477), 359–378.
- GNEITING T, AND RANJAN R (2011), “Comparing density forecasts using threshold-and quantile-weighted scoring rules,” *Journal of Business & Economic Statistics* **29**(3), 411–422.
- HAHN PR, AND CARVALHO CM (2015), “Decoupling Shrinkage and Selection in Bayesian Linear Models: A Posterior Summary Perspective,” *Journal of the American Statistical Association* **110**(509), 435–448.
- HANSEN PR, LUNDE A, AND NASON JM (2011), “The model confidence set,” *Econometrica* **79**(2), 453–497.
- HAUZENBERGER N, HUBER F, AND KOOP G (2020a), “Dynamic Shrinkage Priors for Large Time-varying Parameter Regressions using Scalable Markov Chain Monte Carlo Methods,” *arXiv preprint arXiv:2005.03906* .
- HAUZENBERGER N, HUBER F, KOOP G, AND ONORANTE L (2019), “Fast and Flexible Bayesian Inference in Time-varying Parameter Regression Models,” *arXiv preprint arXiv:1910.10779* .
- HAUZENBERGER N, HUBER F, AND ONORANTE L (2020b), “Combining Shrinkage and Sparsity in Conjugate Vector Autoregressive Models,” *Journal of Applied Econometrics* **forthcoming**.
- HAUZENBERGER N, HUBER F, PFARRHOFER M, AND ZÖRNER TO (2020c), “Stochastic model specification in Markov switching vector error correction models,” *Studies in Nonlinear Dynamics & Econometrics* (in press).
- HOULLIER MA, AND DE MENEZES LM (2012), “A fractional cointegration analysis of European electricity spot prices,” in “9th International Conference on the European Energy Market,” .
- HUBER F, KOOP G, AND ONORANTE L (2020a), “Inducing sparsity and shrinkage in time-varying parameter models,” *Journal of Business & Economic Statistics* (in press).
- HUBER F, KOOP G, AND PFARRHOFER M (2020b), “Bayesian inference in high-dimensional time-varying parameter models using integrated rotated Gaussian approximations,” *arXiv preprint arXiv:2002.10274* .
- HUBER F, AND ZÖRNER TO (2019), “Threshold cointegration in international exchange rates: a Bayesian

- approach,” *International Journal of Forecasting* **35**(2), 458–473.
- JOCHMANN M, AND KOOP G (2015), “Regime-switching cointegration,” *Studies in Nonlinear Dynamics & Econometrics* **19**(1), 35–48.
- JOCHMANN M, KOOP G, LEON-GONZALEZ R, AND STRACHAN RW (2013), “Stochastic search variable selection in vector error correction models with an application to a model of the UK macroeconomy,” *Journal of Applied Econometrics* **28**(1), 62–81.
- KASTNER G (2016), “Dealing with stochastic volatility in time series using the R package stochvol,” *Journal of Statistical software* **69**(5), 1–30.
- KASTNER G, AND FRÜHWIRTH-SCHNATTER S (2014), “Ancillarity-sufficiency interweaving strategy (ASIS) for boosting MCMC estimation of stochastic volatility models,” *Computational Statistics & Data Analysis* **76**, 408–423.
- KLEIBERGEN F, AND VAN DIJK HK (1994), “On the shape of the likelihood/posterior in cointegration models,” *Econometric Theory* **10**(3-4), 514–551.
- (1998), “Bayesian simultaneous equations analysis using reduced rank structures,” *Econometric Theory* **14**(6), 701–743.
- KOOP G, LEÓN-GONZÁLEZ R, AND STRACHAN RW (2009), “Efficient posterior simulation for cointegrated models with priors on the cointegration space,” *Econometric Reviews* **29**(2), 224–242.
- KOOP G, LEON-GONZALEZ R, AND STRACHAN RW (2011), “Bayesian inference in a time varying cointegration model,” *Journal of Econometrics* **165**(2), 210–220.
- LIU JS, AND WU YN (1999), “Parameter expansion for data augmentation,” *Journal of the American Statistical Association* **94**(448), 1264–1274.
- MAKALIC E, AND SCHMIDT DF (2015), “A simple sampler for the horseshoe estimator,” *IEEE Signal Processing Letters* **23**(1), 179–182.
- MEINSHAUSEN N, AND BÜHLMANN P (2006), “High-dimensional graphs and variable selection with the lasso,” *The Annals of Statistics* **34**(3), 1436–1462.
- PAAP R, AND VAN DIJK HK (2003), “Bayes estimates of Markov trends in possibly cointegrated series: An application to US consumption and income,” *Journal of Business & Economic Statistics* **21**(4), 547–563.
- POLSON NG, AND SCOTT JG (2010), “Shrink globally, act locally: Sparse Bayesian regularization and prediction,” *Bayesian statistics* **9**, 501–538.
- PUELZ D, HAHN PR, AND CARVALHO CM (2020), “Portfolio selection for individual passive investing,” *Applied Stochastic Models in Business and Industry* **36**(1), 124–142.
- PUELZ D, HAHN PR, CARVALHO CM, *et al.* (2017), “Variable selection in seemingly unrelated regressions with random predictors,” *Bayesian Analysis* **12**(4), 969–989.
- RAVIV E, BOUWMAN KE, AND VAN DIJK D (2015), “Forecasting day-ahead electricity prices: Utilizing hourly prices,” *Energy Economics* **50**, 227–239.
- RAY P, AND BHATTACHARYA A (2018), “Signal Adaptive Variable Selector for the Horseshoe Prior,” *arXiv preprint arXiv:1810.09004*.
- STRACHAN RW (2003), “Valid Bayesian estimation of the cointegrating error correction model,” *Journal of Business & Economic Statistics* **21**(1), 185–195.
- STRACHAN RW, AND INDER B (2004), “Bayesian analysis of the error correction model,” *Journal of Econometrics* **123**(2), 307–325.
- VILLANI M (2001), “Bayesian prediction with cointegrated vector autoregressions,” *International Journal of Forecasting* **17**(4), 585–605.
- (2006), “Bayesian point estimation of the cointegration space,” *Journal of Econometrics* **134**(2), 645–664.
- (2009), “Steady-state priors for vector autoregressions,” *Journal of Applied Econometrics* **24**(4), 630–650.
- WANG H, AND LENG C (2008), “A note on adaptive group Lasso,” *Computational Statistics & Data Analysis* **52**(12), 5277–5286.
- WERON R (2014), “Electricity price forecasting: A review of the state-of-the-art with a look into the future,” *International Journal of Forecasting* **30**(4), 1030 – 1081.
- WOODY S, CARVALHO CM, AND MURRAY JS (2020), “Model interpretation through lower-dimensional posterior summarization,” *Journal of Computational and Graphical Statistics* **0**(just-accepted).
- YANG Y, AND BAUWENS L (2018), “State-space models on the Stiefel manifold with a new approach to nonlinear filtering,” *Econometrics* **6**(4), 48.
- YUAN M, AND LIN Y (2006), “Model selection and estimation in regression with grouped variables,” *Journal of the Royal Statistical Society: Series B (Statistical Methodology)* **68**(1), 49–67.
- ZOU H (2006), “The adaptive Lasso and its oracle properties,” *Journal of the American Statistical Association* **101**(476), 1418–1429.

A. ECONOMETRIC APPENDIX

A.1. Non-centered parameterization

We rewrite Eqs. (2)–(3) using the non-centered parameterization proposed by [Frühwirth-Schnatter and Wagner \(2010\)](#):

$$\Delta y_{it} = (\mathbf{b}'_{i0} + \tilde{\mathbf{b}}'_{it} \sqrt{\boldsymbol{\Theta}_i}) \mathbf{Z}_{it} + \eta_{it}.$$

Here, $\sqrt{\boldsymbol{\Theta}_i} = \text{diag}(\sqrt{\boldsymbol{\theta}_i})$ with $\sqrt{\boldsymbol{\theta}_i} = (\sqrt{\theta_{i1}}, \dots, \sqrt{\theta_{iK_i}})'$ collecting the standard deviations of the random walk state equation and $\tilde{\mathbf{b}}_{it} = (\mathbf{b}_{it} - \mathbf{b}_{i0})(\sqrt{\boldsymbol{\Theta}_i})^{-1}$ are the normalized states with

$$\tilde{\mathbf{b}}_{it} = \tilde{\mathbf{b}}_{it-1} + \tilde{\boldsymbol{\vartheta}}_{it}, \quad \tilde{\boldsymbol{\vartheta}}_t \sim \mathcal{N}(\mathbf{0}, \mathbf{I}_{K_i}),$$

with $\tilde{\mathbf{b}}_{i0} = \mathbf{0}_{K_i}$. This reparameterization splits the autoregressive coefficients and covariances into a time-invariant and TVP part, and moves the state innovation variances to the observation equation. We collect the time-invariant coefficients and the square root of the state innovation variances in a $2K_i \times 1$ -vector $\hat{\mathbf{b}}_i = (\mathbf{b}'_{i0}, \sqrt{\boldsymbol{\theta}_i}')'$ and the respective covariates in a $2K_i \times 1$ -vector $\tilde{\mathbf{Z}}_{it} = (\mathbf{Z}'_{it}, (\mathbf{Z}_{it} \odot \tilde{\mathbf{b}}_{it})')'$ with \odot denoting the Hadamard product.

A.2. Heavy tailed error distribution

To provide estimates for errors η_{it} specified to follow a t-distribution with ν_i degrees of freedom, we assume

$$\eta_{it} \sim t_{\nu_i}(0, h_{it}), \tag{A.1}$$

where the state equation of h_{it} is given by Eq. (4). Introducing auxiliary variables τ_{it} for $t = 1, \dots, T$ enables to rewrite Eq. (A.1) as conditionally Gaussian:

$$\begin{aligned} \eta_{it} &\sim \mathcal{N}(0, \tau_{it} h_{it}), \\ \tau_{it} &\sim \mathcal{G}^{-1}(\nu_i/2, \nu_i/2). \end{aligned}$$

A.3. Prior distributions

1. On $\hat{\mathbf{b}}_i = (\mathbf{b}'_{i0}, \sqrt{\boldsymbol{\theta}_i}')'$, for $i = 1, \dots, M$, we use a horseshoe prior ([Polson and Scott, 2010](#)). Following [Makalic and Schmidt \(2015\)](#) this hierarchical global-local shrinkage prior can be written as:

$$\hat{b}_{ij} | \psi_{ij}, \varrho_{ik} \sim \mathcal{N}(0, \psi_{ij} \varrho_{ik}), \quad \psi_{ij} \sim \mathcal{IG}(1/2, 1/\rho_{ij}), \quad \varrho_{ik} \sim \mathcal{IG}(1/2, 1/\varpi_{ik}),$$

for $j = 1, \dots, 2K_i$, with $k \in \{b, \theta\}$ indicating group-specific global shrinkage parameters differentiating between \mathbf{b}_{i0} and $\sqrt{\boldsymbol{\theta}_i}$. Both ρ_{ij} and ϱ_{ik} refer to a set of auxiliary variables,

which also follow an inverse Gamma distribution,

$$\rho_{ij} \sim \mathcal{IG}(1/2, 1) \quad \text{and} \quad \varpi_{ik} \sim \mathcal{IG}(1/2, 1).$$

2. Following, [Koop *et al.* \(2009\)](#), the prior on the transformed time-invariant cointegration vectors $\tilde{\beta}$ is

$$\tilde{\beta}_v = \text{vec}(\tilde{\beta}) \sim \mathcal{N}(\mathbf{0}, s_0 \mathbf{I}_{Mq}),$$

with $s_0 = 0.1$ being a weakly informative choice. Here it is worth noting, that similar to [Chakraborty *et al.* \(2020\)](#) we refrain of using another shrinkage prior on elements in $\tilde{\beta}$, due to the multiplicative and non-identified structure of $\mathbf{\Pi}_t = \tilde{\alpha}_t \tilde{\beta}'$.

3. For the stochastic volatility component we follow [Kastner and Frühwirth-Schnatter \(2014\)](#) and specify: $\mu_i \sim \mathcal{N}(0, 100)$, $(\phi_i + 1)/2 \sim \mathcal{B}(5, 1.5)$ and $\varsigma_i \sim \mathcal{N}(0, 1)$, where \mathcal{B} denotes the Beta distribution. The prior on the initial states is $h_{i0} \sim \mathcal{N}(\mu_i, \varsigma_i^2/(1 - \phi_i))$.

A.4. Posterior distributions and algorithm

1. Conditional on all other parameters (denoted by \bullet) draw $\hat{\mathbf{b}}_i$, for $i = 1, \dots, M$, from a multivariate Gaussian distribution:

$$\hat{\mathbf{b}}_i | \bullet \sim \mathcal{N}(\bar{\mathbf{b}}_i, \bar{\mathbf{V}}_i).$$

Let $\hat{\mathbf{y}}_i$ be a $T \times 1$ -vector with the t th element given by $\Delta y_{it}/\sqrt{h_{it}}$, $\hat{\mathbf{Z}}_i$ be a $T \times 2K_i$ -matrix of covariates with the t th row given by $\tilde{\mathbf{Z}}_{it}'/\sqrt{h_{it}}$, and define the prior variance matrix $\underline{\mathbf{V}}_i = \text{diag}(\mathbf{v}_i)$ with $\mathbf{v}_i = (\varrho_{ib}\psi_{i1}, \dots, \varrho_{i\theta}\psi_{i2K_i})$, then the posterior moments are given by:

$$\begin{aligned} \bar{\mathbf{V}}_i &= \left(\hat{\mathbf{Z}}_i' \hat{\mathbf{Z}}_i + \underline{\mathbf{V}}_i^{-1} \right)^{-1}, \\ \bar{\mathbf{b}}_i &= \bar{\mathbf{V}}_i \left(\hat{\mathbf{Z}}_i' \hat{\mathbf{y}}_i \right). \end{aligned}$$

2. Draw the local shrinkage parameters $\{\rho_{ij}\}_{j=1}^{2K_i}$ from

$$\rho_{ij} | \bullet \sim \mathcal{IG} \left(1, \psi_{ij}^{-1} + \frac{\hat{b}_{ij}^2}{2\varrho_{ik}} \right),$$

with $k \in \{b, \theta\}$ selected depending whether j indicates elements of the constant part of the regression coefficients or the square root of the state innovation variances.

3. Draw the global shrinkage parameter ϱ_{ik} for $k \in \{b, \theta\}$:

$$\varrho_{ib}|\bullet \sim \mathcal{IG}\left(\frac{K_i+1}{2}, \varpi_{ib}^{-1} + \frac{1}{2} \sum_{j=1}^{K_i} \hat{b}_{ij}^2 \rho_{ij}^{-1}\right),$$

$$\varrho_{i\theta}|\bullet \sim \mathcal{IG}\left(\frac{K_i+1}{2}, \varpi_{i\theta}^{-1} + \frac{1}{2} \sum_{j=(K_i+1)}^{2K_i} \hat{b}_{ij}^2 \rho_{ij}^{-1}\right).$$

4. Update the auxiliary variables associated with the horseshoe prior (see Makalic and Schmidt, 2015, for details).
5. Draw the normalized time-varying states $\tilde{\mathbf{b}}_{it}$, for $i = 1, \dots, M$, with a forward filtering backward sampling algorithm (Carter and Kohn, 1994; Frühwirth-Schnatter, 1994).
6. Draw the transformed cointegration vectors $\tilde{\boldsymbol{\beta}}_v$ from a multivariate Gaussian distribution:

$$\tilde{\boldsymbol{\beta}}_v|\bullet \sim \mathcal{N}(\bar{\boldsymbol{\beta}}_v, \bar{\mathbf{V}}_\beta).$$

Let $\ddot{\mathbf{y}}$ be a $T \times M$ -matrix with $\ddot{\mathbf{y}}'_t = (\Delta \mathbf{y}_t - \mathbf{A}_t \mathbf{x}_t)' \boldsymbol{\Sigma}_t^{-0.5'}$ on the t th position and $\ddot{\mathbf{X}}$ a $TM \times Mq$ -matrix with t th block given by $\ddot{\mathbf{x}}_t = (\mathbf{y}'_{t-1} \otimes \boldsymbol{\Sigma}_t^{-0.5} \tilde{\boldsymbol{\alpha}}_t)$, then the posterior moments are given by:

$$\bar{\mathbf{V}}_\beta = (\ddot{\mathbf{X}}' \ddot{\mathbf{X}} + 1/s_0 \mathbf{I}_{Mq})^{-1},$$

$$\bar{\boldsymbol{\beta}}_\beta = \bar{\mathbf{V}}_\beta \ddot{\mathbf{X}}' \text{vec}(\ddot{\mathbf{y}}).$$

7. Draw the time-varying volatilities h_{it} , for $i = 1, \dots, M$, and the parameters of the state equation using the **R** package `stochvol` (Kastner, 2016). This step involves drawing the degrees of freedom parameter for the t-distribution in the case of heavy tailed errors.
8. Finally, we perform sparsification for each draw as outlined in detail in Section 2.2.